Cryogenic etching of silicon with SF6 inductively coupled plasmas: a combined modelling and experimental study

Stefan Tinck, Thomas Tillocher, Rémi Dussart, Annemie Bogaerts

Cryogenic etching of silicon with SF_6 inductively coupled plasmas: a combined modelling and experimental study

Reference:

Tinck Stefan, Tillocher Thomas, Dussart Rémi, Bogaerts Annemie.- Cryogenic etching of silicon with SF_6 inductively coupled plasmas: a combined modelling and experimental study

Journal of physics: D: applied physics - ISSN 0022-3727 - 48:15(2015), 155204

DOI: http://dx.doi.org/doi:10.1088/0022-3727/48/15/155204

Cryogenic etching of silicon with SF_6 inductively coupled plasmas: A combined modelling and experimental study

Stefan Tinck[1], Thomas Tillocher[2], Rémi Dussart[2] and Annemie Bogaerts[1]

[1]Research Group PLASMANT, Dept. of Chemistry, University of Antwerp, Universiteitsplein 1, B-2610 Antwerp, Belgium

[2]GREMI, CNRS/Université d'Orléans, Rue d'Issoudun 14, BP 6744, F-45067 Orléans, France

Abstract. A hybrid Monte Carlo - fluid model is applied to simulate the wafer-temperature-dependent etching of silicon with SF_6 inductively coupled plasmas. The bulk plasma within the ICP reactor volume as well as the surface reactions occurring at the wafer are self-consistently described. The calculated etch rates are validated by experiments. The calculations and experiments are performed at two different wafer temperatures, i.e., 300 K and 173 K, resembling conventional etching and cryoetching, respectively. In the case of cryoetching, a physisorbed SF_x layer (x=0-6) is formed on the wafer, which is negligible at room temperature, because of fast thermal desorption, However, even in the case of cryoetching, this layer can easily be disintegrated by low-energy ions, so it does not affect the etch rates. In the investigated pressure range of 1 to 9 Pa, the etch rate is always slightly higher at cryogenic conditions, both in the experiments and in the model, and this could be explained in the model due to a local cooling of the gas above the wafer, making the gas denser and increasing the flux of reactive neutrals, like F and F_2, towards the wafer.

I. Introduction

Plasma etching is a powerful technique for transferring lithographic masks with nanoscale resolution into functional materials.[1] Recently, deep reactive ion etching (DRIE) of silicon is needed for creating silicon vias and 3D microelectronic components. In this process, trenches or holes are etched in silicon with an extremely high aspect ratio. There are two main technologies for fast DRIE: the Bosch

process and cryogenic etching. During the Bosch process, a passivating gas (e.g. C_4F_8) and etching gas (e.g. SF_6) are alternated.[2] Disadvantages of the Bosch process are the relatively expensive C_4F_8 gas, the scalloped sidewalls and contamination of the reactor walls. These disadvantages are absent for cryogenic etching.

In silicon cryoetching, first proposed in 1988 by Tachi[3], the wafer is cooled to −100 °C and a SF_6/O_2 mixture is applied. During cryogenic DRIE, a SiF_xO_y passivation layer is formed which prevents isotropic etching. When the wafer is heated to room temperature, this passivation layer desorbs naturally, leaving a clean trench with no scalloping.[4] The primary issue with cryogenic DRIE is the high sensitivity to oxygen content and substrate temperature. Also the mask can crack under the extreme cold and etch products have a higher tendency to deposit on the cold substrate.

In recent years, silicon cryoetching is gaining increasing interest. However, the underlying mechanisms of how the SiF_xO_y passivation layer is formed and automatically desorbs at higher temperature are not yet fully understood, and in particular the issue of how to control critical dimensions of microstructures is still unresolved.[5] A recent topical review by Dussart *et al.*[5] covers the latest advances in cryoetching, ranging back from the origin of cryoetching to today's technologies. The interested reader is referred to this review for a detailed overview of cryogenic etching.

Although the list of experimental papers on cryoetching is tremendous, modeling studies on cryoetching are still very limited. Blauw *et al.*[6] have investigated the kinetics of SF_6/O_2 anisotropic silicon etching with a Monte Carlo surface model and experiments. Their modeling work was limited to the surface interactions only, so no gas phase plasma calculations were performed. Marcos and Rhallabi[7] also performed Monte Carlo etch profile simulations with SF_6/O_2 to investigate the profile evolution during etching. They varied the F sticking coefficient and compared the calculated profile with SEM pictures to determine the overall sticking probability for F atoms.

The goal of our work is to determine the fundamental differences in etching at cryogenic conditions compared to room temperature when using pure SF_6 to etch silicon. In practice, O_2 is always added to SF_6 to create the passivation layer. However, as will be demonstrated below, using only SF_6 will already yield slightly different etch rates as a function of temperature. We believe that understanding

the temperature-dependent surface behavior of the F atoms to etch silicon is a primary step in obtaining full insight in the mechanisms of the SiF_xO_y passivation layer formation and automatic desorption. Furthermore, we also want to elucidate how the plasma might be affected by different wafer temperatures. For this purpose, we apply a self-consistent model that covers both the bulk plasma characteristics as well as the surface processes during etching. For validation of the modeling results, the etch rates are also experimentally obtained with reflectometry.

The description of the model as well as the constructed reaction set defined in the model are presented in section II, while the experimental setup is explained in section III. The modeling and experimental results are discussed in section IV.

II. Computational details

The so-called hybrid plasma equipment model (HPEM), developed by Kushner, is applied to describe the plasma processes and plasma-surface interactions.[8] This model calculates the plasma characteristics in a two-dimensional cross section of the cylindrical reactor, by combining a Monte Carlo method for the electrons and a fluid simulation for all other plasma species. It consists of an electromagnetics module, where the electromagnetic fields are calculated by solving Maxwell's equations, an electron Monte Carlo module, where the electron properties are determined, and a fluid part, which treats the heavy plasma species. A more detailed explanation of the model can be found in this reference.[8]

Furthermore, the model includes an analytical module to address the plasma-surface interactions. More specifically, the fluxes of all plasma species to the reactor walls and wafer are input in this module, to describe the etching process based on a predefined surface chemistry reaction set. From this module, the fluxes of species returning to the plasma are defined for an updated description of the plasma chemistry. The overall calculation switches between these two models in an iterative way until convergence is reached.

The predefined surface reaction set needs surface reaction probabilities, i.e., sticking probabilities and sputter yields, as input. These probabilities were obtained from Molecular Dynamics (MD) simulations, carried out in a previous study.[10] To perform the MD simulations, different slabs of atoms were created with varying chemical compositions ranging from Si(100) to SiF_3. The relevant plasma species were then launched towards these surfaces for many impacts to calculate the sticking and sputter probabilities. The fluxes, kinetic energies and angles of bombardment were generated by the HPEM and were defined in the MD simulations. In turn, the calculated sticking and sputter probabilities from the MD simulations are implemented in the surface reaction set of the analytical surface module of the HPEM.

In the following sections, we present an overview of the different plasma species included in the model and the surface chemistry reaction set. The gas phase reaction set for an SF_6 plasma etching silicon was adopted from Mao *et al.*[9] and is not repeated here.

1. Species considered in the model

27 different plasma species are taken into account for describing the SF_6 plasma chemistry, as well as 11 different surface layers (also called "surface species") for addressing the etching process. The complete list of species is shown in **Table 1**.

Table 1. Overview of the species included in the model. Species denoted with "(s)" should be interpreted as chemical compositions of the surface.

Neutral species:	SF_6, SF_5, SF_4, SF_3, SF_2, SF, S, F, F_2, F*, SiF_4
Charged species:	SF_5^+, SF_4^+, SF_3^+, SF_2^+, SF^+, S^+, F^+, F_2^+
	SF_6^-, SF_5^-, SF_4^-, SF_3^-, SF_2^-, F^-, SiF_4^-, free electrons
Surface species:	$Si_{(s)}$, $SiF_{(s)}$, $SiF_{2(s)}$, $SiF_{3(s)}$, $SF_{6(s)}$, $SF_{5(s)}$, $SF_{4(s)}$, $SF_{3(s)}$, $SF_{2(s)}$, $SF_{(s)}$, $S_{(s)}$

2. Surface reaction set

In a previous paper by Tinck et al.[10], we determined sticking coefficients for fluorine species on silicon as a function of the chemical composition of the surface, both at room temperature and

cryogenic conditions, by means of molecular dynamics (MD) simulations. Furthermore, the formation of a physisorbed layer on the wafer was predicted by the MD simulations, and the corresponding thermal desorption rates, both at room temperature and cryogenic conditions, were calculated. The obtained sticking probabilities and thermal desorption rates of the physisorbed layer are adopted here and presented in **Table 2**, along with the probabilities for formation and removal of the physisorbed layer, as treated in the present model.

Table 2. Schematic overview of the surface reactions defined in the model. The different reaction types are shown in the left column, with the corresponding probabilities or rates in the right column. The sticking probabilities (fluorination of silicon; process 1) and the rates for thermal desorption (process 3) are adopted from reference[10], while the probabilities for formation of the physisorbed layer and removal by ions (processes 2 and 4, respectively) are described directly in the present model (see text). Species with a "(s)" subscript denote surface layers and those with a "(phys)" subscript are part of a physisorbed layer that can accumulate on the surface during etching. M^+ comprises all possible positive ions as listed in **Table 1**.

1. Fluorination of silicon	
$F + SiF_{x(s)}$ (x = 0-3) → $SiF_{x+1(s)}$	0.98 / 0.93 / 0.59 / 0.23 (for x = 0 / 1 / 2 / 3) [a, b]
$F_2 + SiF_{x(s)}$ (x = 0-3) → $SiF_{x+1(s)} + F$	1.00 (for x = 0-3) [a, b]
2. Formation of a physisorbed layer	
SF_x (x = 0-6) + $surface_{(s)}$ → $SF_{x(phys)}$	$1/(1 + 0.3[\text{Physisorbed layer coverage}])^2$ [c]
3. Thermal desorption of physisorbed species	
$SF_{x(phys)}$ (x = 0-6) → SF_x	0.001 s^{-1} (for cryogenic etching; 173 K) 14285 s^{-1} (for room temp. etching; 300 K)
4. Removal of the physisorbed layer by ions	
$M^+ + SF_{x(phys)}$ (x = 0-6) → $M + SF_x$	Equal to physisorbed layer coverage [d]

[a] In the case of x = 3, SiF_4 is formed, which is considered volatile; hence this is the actual etching step.
[b] The sticking probabilities are found to be the same for cryogenic etching and room temperature etching.
[c] $surface_{(s)}$ comprises all possible surface layers as listed in **Table 1**. For the explanation of the formula: see text.
[d] The probability is equal to the physisorbed layer coverage, to make sure that the ions completely disintegrate the physisorbed layer. For more details: see text.

In the MD simulations, all the structures were thermalized at 300 K or 173 K employing a Berendsen heat bath with a coupling constant of 100 fs. However, our MD simulations predicted that the sticking

probabilities of F atoms on a (fluorinated) silicon surface are identical at 173 K and 300 K. The difference in kinetic energy between both temperatures is simply too small to have a significant effect on the rate for chemisorption. The sticking probabilities decrease with an increasing degree of fluorination because fewer sites for chemisorption are available when the surface is highly fluorinated. Because the F atoms are relatively light, our MD simulations revealed that they always either chemisorb, or become immediately reflected from the surface, and they never stay physisorbed along the surface for a significant amount of time.[10]

The F_2 molecules are also very reactive towards the silicon surface. Due to their weak bond strength (1.60 eV), they easily dissociate upon arrival at the surface, and usually one F atom chemisorbs while the other accepts the remaining energy of the reaction as a fast neutral and is reflected from the surface. Because the F_2 molecules are twice as heavy as the F atoms, they undergo stronger dispersion forces, keeping them longer along the surface before thermal desorption occurs, increasing the chance for eventual chemisorption. For this reason, the sticking probabilities of the F_2 molecules were calculated to be higher than those of the F atoms; more specifically, they were equal to 1 for all surfaces, both at 173 and 300 K.[10]

Although the sticking probabilities (i.e., chemisorption) of F atoms and F_2 molecules are the same for room temperature etching and cryoetching, the behaviour of the physisorbed species along the surface is different in both cases. The thermal desorption rate of physisorbed species depends both on the activation energy for desorption and on the temperature. At cryoetching, the activation energy is slightly higher due to stronger average dispersion forces, and in combination with the lower kinetic energy of the species to overcome the barrier, this results in a much longer residence time compared to room temperature etching; cf. the thermal desorption rates, predicted by the MD simulations for both temperatures, as shown in **Table 2**. As a result, there is a significant difference in the thickness (or coverage) of the physisorbed layer grown during etching at both temperatures, as will be illustrated in section IV below. More specifically, at cryogenic temperature, this layer can be quite thick, while at room temperature, the formation of a physisorbed layer is negligible, because of the much higher thermal desorption rate.

The actual thickness of the physisorbed layer in the case of cryoetching could, however, not be determined with our MD simulations, because the layer becomes too thick to completely capture with MD. However, we do know that the physisorbed layer becomes less dense when moving away from the underlying silicon. Hence, further accumulation becomes slower and is eventually limited at a certain thickness, and this is described in the present model by a probability for formation of this layer which is function of the physisorbed layer coverage, as shown in **Table 2**. This is a predefined equation, hard-coded in the plasma model[8] that properly captures the physics of thickness limited growth of a physisorbed layer, as observed in our MD simulations. Although the formula captures the growth mechanism in a proper way, it does not yield the real thickness, which could not be obtained from MD and is hence an unknown factor. The thicknesses, or better the coverage, of the physisorbed layers obtained at both temperatures can therefore be compared only qualitatively, as will be illustrated in section IV below.

The fundamental difference between cryoetching and room temperature etching is thus the formation of this physisorbed layer. At room temperature, this layer is also formed, but it is almost immediately removed again by thermal desorption, while at cryogenic etching, this layer can be very thick. Indeed, for example at -140 °C (not investigated here), it is known that SF_6 condenses on the surface, creating a macroscopic physisorbed layer with a thickness up to μm-mm scale.[11] It should be realized that the formation of a physisorbed passivation layer will slightly oppose ion sputtering because the ions need to travel through this layer before sputtering the underlying silicon wafer. However, as we do not apply a bias at the wafer in the current investigation, sputtering of the silicon surface by (energetic) ions is not relevant and not considered in the model.

On the other hand, low energy ions can efficiently remove the physisorbed layer, since the molecules that make up the adsorbed layer are not chemically bound to the surface. It was observed in our MD simulations that a thick layer of physisorbed species can be completely removed by ions of 10-20 eV.[10] However, since there are no chemical bonds between the molecules that make up the physisorbed layer, this layer is very dynamic and is always easily removed, even by very-low-energy ions of 1-5 eV as found here (see section IV). The probability for removal of the physisorbed layer by

low-energy ions is therefore defined in our model as being equal to the layer coverage, to ensure that with each ion impact, the layer is completely disintegrated.

To conclude, the physisorbed layer, albeit different in thickness for cryoetching vs room-temperature etching, does not affect the etch rate for both cases, as ion sputtering is irrelevant under the investigated conditions (see section IV), and moreover, during the etching process, low-energy ions will always completely disintegrate the physisorbed layer. However, it is important to realize that this physisorbed layer will always be present in the case of cryoetching, since the flux of neutrals is typically a few orders of magnitude higher compared to the ion flux, so this layer will always be formed again before the next ion arrives to remove it.

III. Experimental

An Alcatel 601E inductively coupled plasma (ICP) reactor is applied for the experiments.[12] A two-dimensional half cross section of this reactor is shown in **figure 1.** The same geometry is also defined in the model. The plane must be rotated along the left Z-axis to obtain the complete cylindrical reactor. The SF_6 gas is fed from the top through the nozzle and the plasma is sustained by the ICP coil surrounding the 200 mm diameter alumina tube powered by an RF power supply at 13.56 MHz. This antenna is surrounded itself by a coil that generates a permanent magnetic field along the z axis of the tube. Underneath the tube is the 400 mm diameter diffusion chamber that allows the reactive plasma species to interact with the wafers. We use 150 mm diameter silicon wafers, which can be independently biased by an RF power supply working at 13.56 MHz. They can be cooled from the bottom by liquid nitrogen through a thin film of helium between the chuck and the wafer. The diffusion chamber is also surrounded by permanent magnets which are placed outside.

The etch rate is measured in situ with double-point reflectometry, which consists of a 650 nm laser diode from which two separate spots can be positioned precisely at different places on the wafer: a point on the mask and one inside a trench. The interacting phase shift between the two reflected beams is recorded to measure the etch rate during the etch process. As the sample is etched, the height

difference between the trench bottom and the mask increases, which makes a succession of constructive and destructive interferences appear. The interference signal is then recorded by a picoscope. The etch rate is computed from the period of the signal which corresponds to an etched thickness of $\lambda/2n$, where λ is the wavelength of the laser diode and n the refractive index of the medium between the mask and the etched trench bottom (n=1 under vacuum). This method thus assumes that the mask is almost not etched.

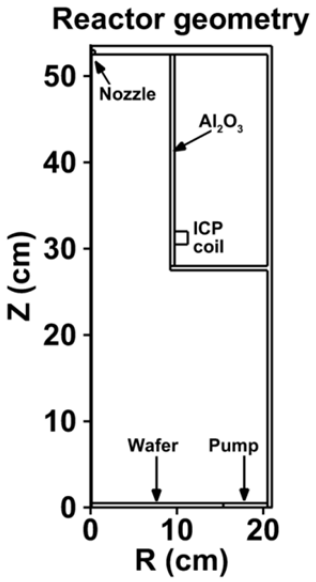

Figure 1. Two-dimensional schematic diagram of the ICP reactor used for the experiments. This is also the geometry defined in the computational model.

IV. Results and Discussion

1. General plasma characteristics

To better understand the surface processes, we first present the general plasma characteristics for the following operating conditions: 13.56 MHz operating frequency, 1000 W ICP power, 150 sccm SF_6 gas flow rate, no substrate bias, a gas pressure of 5 Pa, with a wafer temperature of 173 K. The results

were almost the same at a wafer temperature of 300 K, except for some small differences, discussed in the next section.

Figure 2 shows the density profile of the background gas SF_6, as well as the gas flow lines through the reactor when the plasma is on.

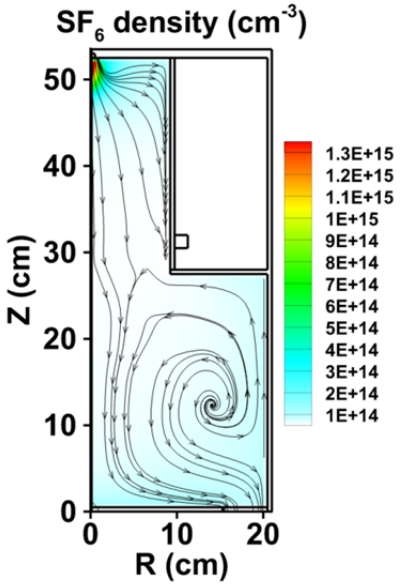

Figure 2. SF_6 density profile and gas flow lines through the reactor, at the conditions mentioned in the text.

SF_6 has the highest density near the nozzle, before it dissociates into SF_x products. About 5 % of the SF_6 gas is dissociated under these conditions. The gas flows from the top nozzle downwards the wafer and to the bottom side where the gas is pumped out. At the top corners near the nozzle and in the diffusion chamber, some recirculation streams may occur, as is clear from the flow lines in **figure 2**.

The density profiles of the F atoms and F_2 molecules, i.e., the most important reactive species for the etching process, are shown in **figure 3**.

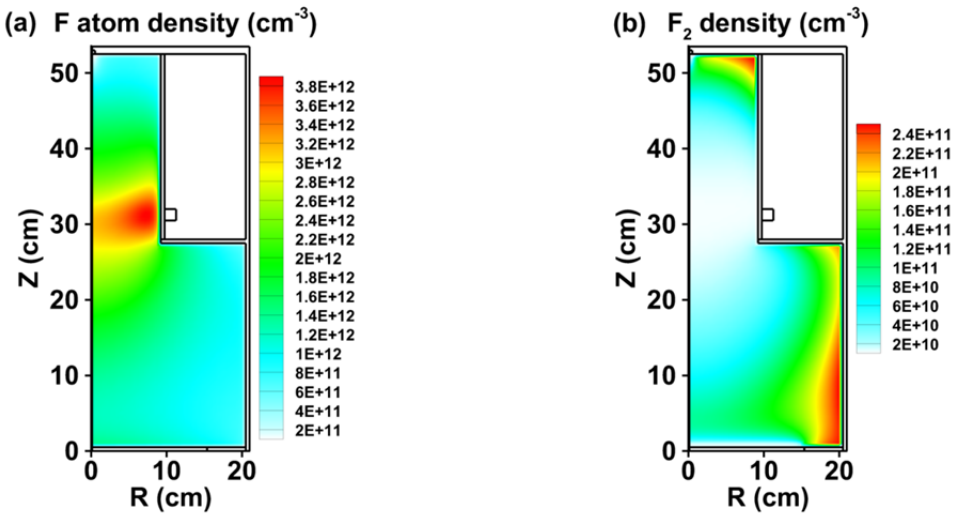

Figure 3. F atom and F_2 molecule density profiles within the reactor volume.

The F atom density has a maximum near the coil, where most dissociation reactions take place. The overall volume averaged density is in the order of 1.2 x 10^{12} cm^{-3}, which is 1.7 % of the volume averaged SF_6 density (i.e., 7.1 x 10^{13} cm^{-3}). All other SF_6 dissociation products, i.e., SF_x (x = 0-5), show similar density profiles, but with lower volume averaged densities, in the order of 10^{9}-10^{11} cm^{-3}. The F_2 volume averaged density is about two orders of magnitude lower than that of F, but it has a density profile comparable to that of SF_6 because it is not a direct product of electron impact dissociation of SF_x (x = 0-6). Indeed, F_2 is created by recombination of F with other gas phase species, or by recombination at the walls, explaining why the F_2 density is found to be at maximum near the walls.

The potential distribution in the plasma is illustrated in **figure 4**, showing a maximum near the coil of about 25 V, where the plasma density is highest. The electromagnetic fields are strongest near the coil, so most ions and free electrons are created in this area, creating the maximum positive potential of 25 V. Near the wafer, however, the plasma potential is near zero, and thus the electric fields are negligible.

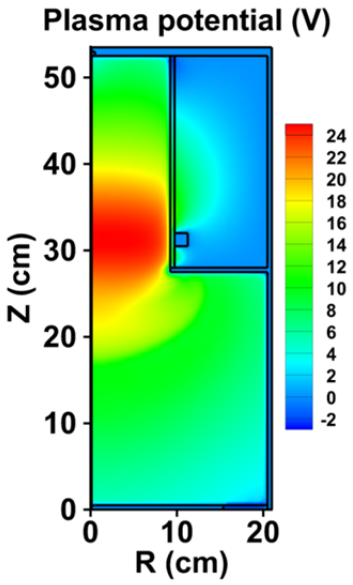

Figure 4. Potential distribution within the reactor volume.

Because the plasma source is relatively far from the wafer, the ion density above the wafer is not very high and the sheath potential is rather low (i.e., order of 1-2 V). Since we don't apply an external bias, most ions thus arrive at the wafer with an energy of less than 2 eV. The energy distributions of the neutral species and ions arriving at the wafer are shown in **figure 5**. These distributions do not vary significantly within the entire investigated pressure range (1 - 9 Pa) and they are also roughly the same for both wafer temperatures. The silicon sputter yield threshold is near 30 eV, so sputtering of the silicon wafer is indeed negligible. The etch rate is thus mainly dependent on the fluxes of the neutral chemical etching species, F and F_2.

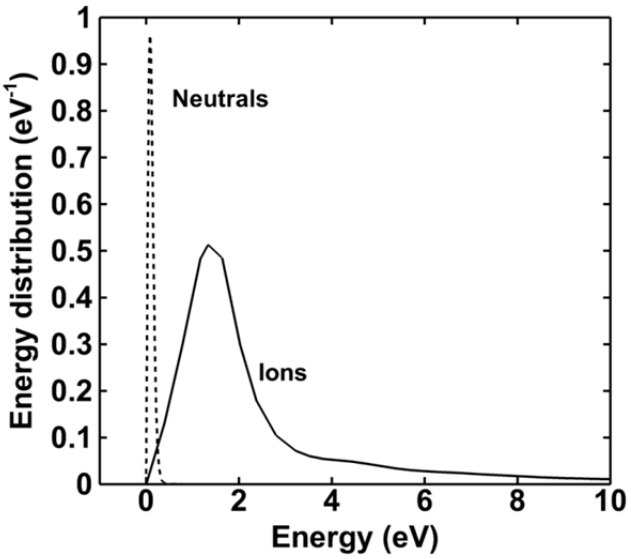

Figure 5. Neutral (dashed) and ion (solid) energy distributions when arriving at the wafer. Both distributions have a Maxwellian shape because there is no external bias applied. Both distributions are normalized so that their areas sum up to one.

2. Differences between room temperature etching and cryoetching

Figure 6(a-d) shows the fluxes of the neutral species (a,b) and the ions (c,d) towards the wafer, as a function of pressure, both for 173 K (a,c) and 300 K (b,d). The F atom flux is clearly higher than the fluxes of the other products, suggesting that the F atoms are indeed the most important species responsible for the etching process.

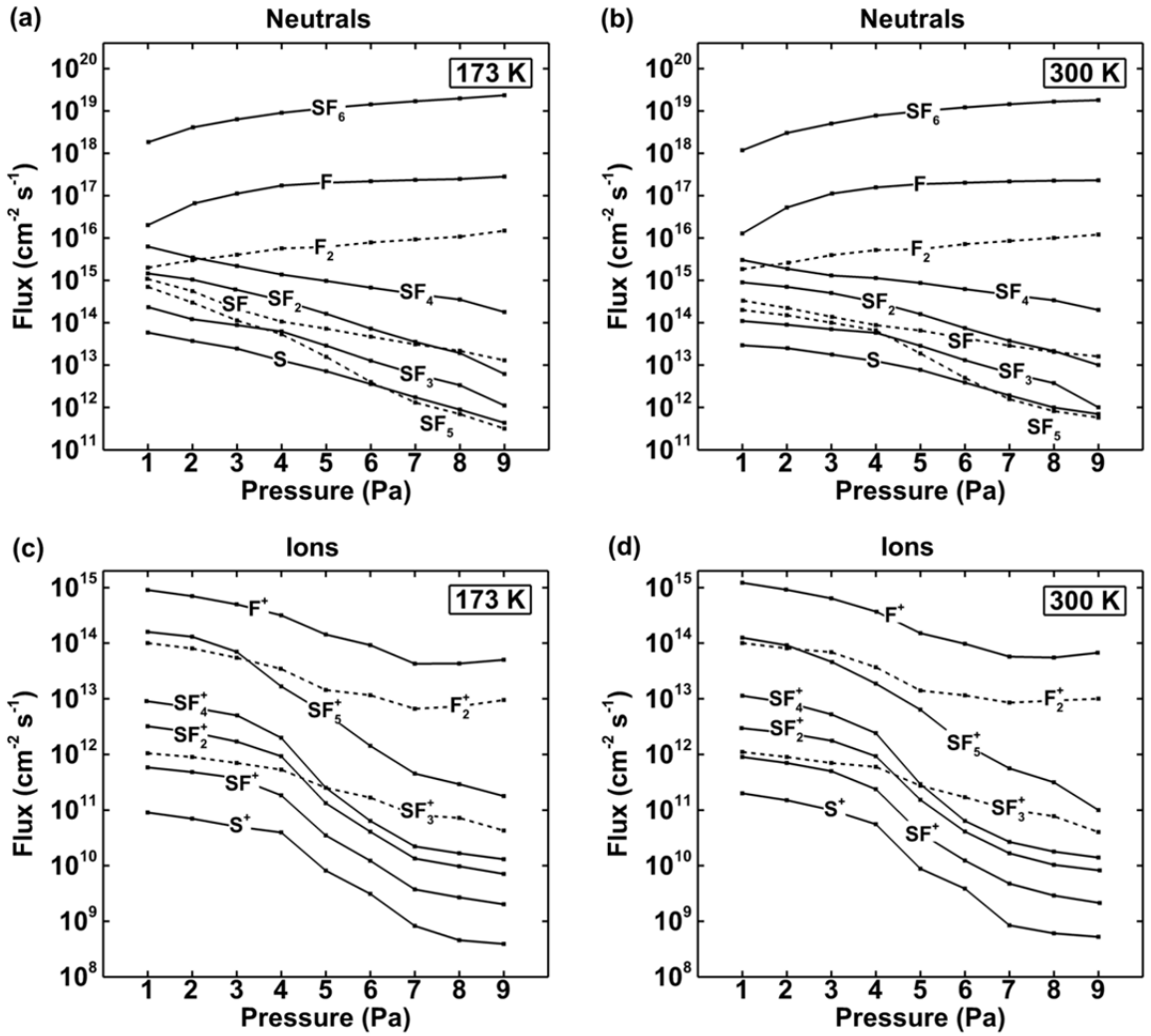

Figure 6. Neutral fluxes towards the center of the wafer, as a function of pressure, at (a) 173 K and (b) 300 K and ion fluxes at (c) 173 K and (d) 300 K. Some lines are dashed for clarity. The fluxes obtained at 173 K and 300 K vary only slightly as further discussed in the text.

The total neutral flux increases with pressure because there are more species present in the reactor. However, due to a higher collision frequency (for among others ion-electron recombination), the ion fluxes tend to decrease as a function of pressure. For the same reason, the fluxes of the SF_x species decrease upon increasing pressure, as recombination reactions tend to lower the fraction of dissociated SF_6.

As mentioned in section II, the sticking probabilities of F and F_2 on silicon are similar for both 173 K and 300 K. The difference is found in the thickness of the physisorbed layer, as was also predicted by our MD simulations.[9] Note that the absolute thickness could not be obtained in the model, but instead,

the model provides the coverage of this physisorbed layer, which is illustrated in **figure 7**. Note that a coverage above 1 indicates that more than one physisorbed monolayer is formed. It is clear that the physisorbed layer is several orders of magnitude thicker at cryogenic temperature than at room temperature. Indeed, at 300 K, the thermal desorption rate is high enough to ensure that the wafer surface is only covered with physisorbed SF_x species (x = 0-6) for less than 1 % (hence, significantly less than one monolayer) under all investigated pressures. On the other hand, at 173 K, the physisorbed layer has a significant thickness (corresponding to more than one monolayer), due to the slower thermal desorption. The thickness increases with pressure, because the ratio of neutral-to-ion flux increases with pressure (see **figure 6** above), indicating that a thicker physisorbed layer can be formed before it is disintegrated by ions.

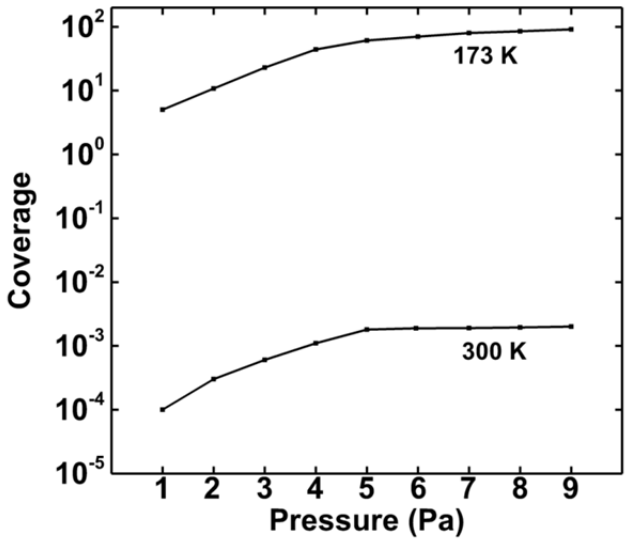

Figure 7. Calculated coverage of the physisorbed layer on the wafer, grown during cryoetching and room temperature etching. A coverage above 1 indicates that more than one monolayer is formed, so it is a (qualitative) measure for the thickness of the physisorbed layer.

As the plasma source is relatively remote from the wafer surface, the plasma itself is not significantly influenced by the wafer temperature. Indeed, all bulk plasma properties are found to be identical in both cases, i.e., for a wafer temperature of 300 K and 173 K. Consequently, the fluxes towards the wafer at 173 K and 300K seem quite similar at first sight (see **figure 6**). However, the gas in the neighborhood of the wafer is locally affected. If the wafer is cooled to 173 K, the gas above the wafer

is colder as well, as illustrated in **figure 8(a)**. This lower gas temperature above the wafer is of course absent for the 300 K wafer, as is clear from **figure 8(b)**.

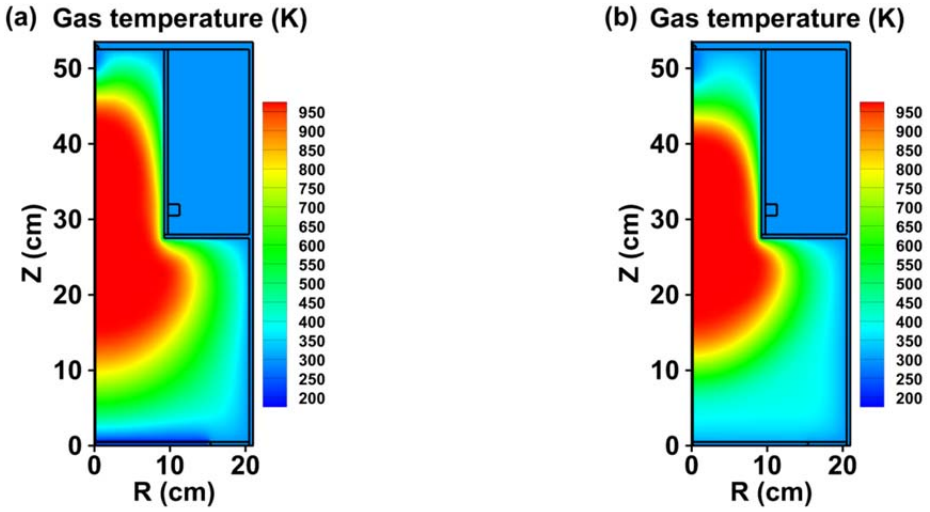

Figure 8. Average gas temperature profiles in the plasma sustained at 5 Pa for a 173 K wafer (a) and 300 K wafer (b). Note the difference in gas temperature right above the wafer.

The local gas temperature drop found during cryoetching entails a slight increase of the neutral species densities near the wafer following the ideal gas law, because the pressure is regulated to be constant during the etching process, and this also affects the neutral fluxes, as illustrated in **figure 9**, together with the (small) difference in total ion flux.

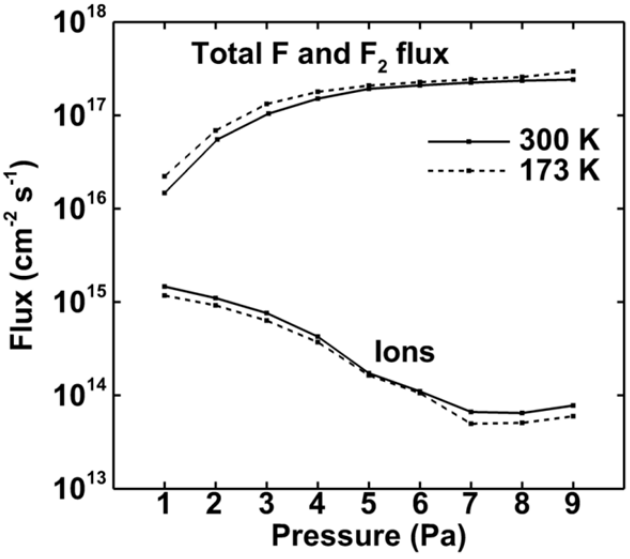

Figure 9. Calculated surface averaged fluxes of F and F_2 towards the wafer in the range of 1 - 9 Pa for 300 K and 173 K wafer temperatures.

The somewhat higher F and F_2 fluxes towards the wafer cause a slightly higher etch rate, as predicted by the model, and this is also observed experimentally, as shown in **Figure 10**. Both calculated and measured etch rates increase with pressure, due to the higher F and F_2 fluxes, and the values at 173 K are indeed slightly higher than at 300 K in both the experiments and the model. The agreement between the measured and calculated etch rates is quite reasonable, showing that the correct physics are captured by the model. Hence, it is clear that the somewhat higher etch rate in cryoetching is due to the local cooling above the wafer, yielding somewhat higher densities and fluxes towards the wafer, and that the physisorbed layer, which is more prominent in the case of cryoetching, does not affect the etch rate, at least when no bias is applied at the wafer.

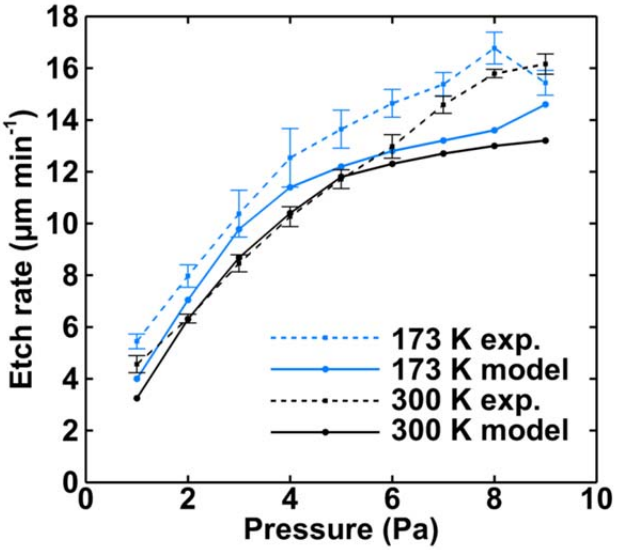

Figure 10. Experimental and calculated etch rates as a function of pressure, for a wafer temperature of 300 K and 173 K.

Finally, the uniformity of the fluxes (or etch rate) along the surface of the wafer is not affected when etching under cryogenic conditions. The best uniformity is found at the lowest pressure of 1 Pa and becomes slightly worse with increasing pressure, but there is no change in quality of the uniformity, comparing the results of 173 K and 300 K. This is illustrated in **Figure 11**, showing the F atom fluxes along the surface, from the center of the wafer to the edge for 1 Pa, 4 Pa and 9 Pa and for both 173 K and 300 K.

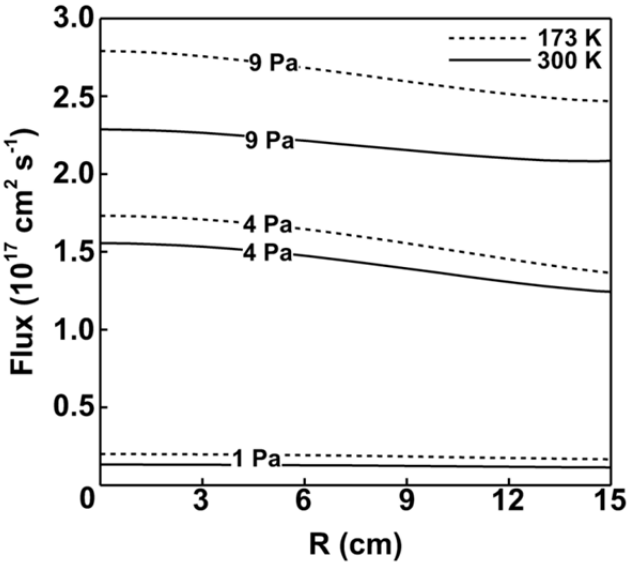

Figure 11. Calculated F fluxes along the wafer surface, from the center (x = 0 cm) to the edge (x = 15 cm) of the wafer.

V. Conclusions

We have numerically investigated an SF_6 low-pressure ICP, at two different wafer temperatures of 300 K and 173 K, to better understand the difference between cryoetching and room temperature etching. In this type of ICP reactor, where the plasma source is remote from the wafer, the bulk plasma is unaffected by the wafer temperature. Nevertheless, the experimental etch rates are slightly higher at cryogenic temperature than at room temperature. This could be explained by the model, because the gas is cooled locally above the wafer, resulting in a slightly denser gas and thus a higher density of reactive species, like F and F_2. This in turn entails a slightly higher flux of etching species towards the wafer, resulting in a slightly higher etch rate in the case of cryoetching. The predicted etch rates as a function of pressure, at wafer temperatures of both 300 K and 173 K, are indeed in fairly good agreement with the measured etch rates, suggesting that the correct physics have been captured by the model.

Finally, it is also found that a thick layer of physisorbed species is formed during cryoetching, which is more or less absent at room temperature etching. This layer, however, has no effect on the etch rates because ion sputtering is irrelevant under the investigated conditions (i.e., no external bias) and the physisorbed layer itself is easily disintegrated by low-energy ions.

Acknowledgements

The Fund for Scientific Research Flanders (FWO) is acknowledged for financial support of this work. This work was carried out in part using the Turing HPC infrastructure at the CalcUA core facility of the Universiteit Antwerpen, a division of the Flemish Supercomputer Center VSC, funded by the Hercules Foundation, the Flemish Government (department EWI) and the University of Antwerp.

References

[1] Moore G, *Electronics* **38** 8 1965

[2] Laermer F and Schilp A, *US Patent* 5498312 (assigned to Bosch GmbH) 1996

[3] Tachi S, Tsujimoto K and Okudaira S, *Appl. Phys. Lett*. **52** 616 1988

[4] Dussart R, Boufnichel M, Marcos G, Lefaucheux P, Basillais A, Benoit R, Tillocher T, Mellhaoui X, Estrade-Szwarckopf H and Ranson P, *J. Micromech. Microeng*. **14** 190–196 2004

[5] Dussart R, Tillocher T, Lefaucheux P and Boufnichel M, *J. Phys. D: Appl. Phys*. **47** 123001 2014

[6] Blauw M A, van der Drift E, Marcos G and Rhallabi A, *J. Appl. Phys.* **94** 6311 2003

[7] Marcos G, Rhallabi A and Ranson P, *J. Vac. Sci. Technol.* B **21** 87 2003

[8] Kushner M, *J. Phys. D: Appl. Phys.* **42** 194013 2009

[9] Mao M, Wang YN and Bogaerts A, *J. Phys. D: Appl. Phys.* **44** 435202 2011

[10] Tinck S, Neyts E and Bogaerts A, *J. Phys. Chem. C*, in press, DOI: 10.1021/jp5108872

[11] Bestwick T D, Oehrlein G S and Angell D, *Appl. Phys. Lett.* **57** 431 1990

[12] Boufnichel M, Aachboun S, Lefaucheux P and Ranson P, *J. Vac. Sci. Technol. B* 21(1) 267-273 2003